HHS Public Access

Author manuscript

Cytokine. Author manuscript; available in PMC 2018 August 01.

Published in final edited form as:

Cytokine. 2017 August ; 96: 238–246. doi:10.1016/j.cyto.2017.04.023.

Biochemical and Biophysical Characterization of Cytokine-like Protein 1 (CYTL1)

Aurelie Tomczak[a], **Kavita Singh**[b], **Apostolos G. Gittis**[b], **Joohee Lee**[a], **David N. Garboczi**[b], and **Philip M. Murphy**[a,1]

[a]Molecular Signaling Section, Laboratory of Molecular Immunology, National Institute of Allergy and Infectious Diseases, Rockville, MD 20892, USA

[b]Structural Biology Section, Research Technologies Branch, National Institute of Allergy and Infectious Diseases, Rockville, MD 20852, USA

Abstract

Cytokine-like protein 1 (CYTL1) is a small widely expressed secreted protein lacking significant primary sequence homology to any other known protein. CYTL1 expression appears to be highest in the hematopoietic system and in chondrocytes; however, maintenance of cartilage in mouse models of arthritis is its only reported function in vivo. Despite lacking sequence homology to chemokines, CYTL1 is predicted by computational methods to fold like a chemokine, and has been reported to function as a chemotactic agonist at the chemokine receptor CCR2 in mouse monocyte/macrophages. Nevertheless, since chemokines are defined by structure and chemokine receptors are able to bind many non-chemokine ligands, direct determination of the CYTL1 tertiary structure will ultimately be required to know whether it actually folds as a chemokine and therefore is a chemokine. Towards this goal, we have developed a method for producing functional recombinant human CYTL1 in bacteria, and we provide new evidence about the biophysical and biochemical properties of recombinant CYTL1. Circular dichroism analysis showed that, like chemokines, CYTL1 has a higher content of beta-sheet than alpha-helix secondary structure. Furthermore, recombinant CYTL1 promoted calcium flux in chondrocytes. Nevertheless, unlike chemokines, CYTL1 had limited affinity to proteoglycans. Together, these properties further support cytokine-like properties for CYTL1 with some overlap with the chemokines.

Keywords

structural biology; circular dichroism; recombinant protein; human; chondrocyte; chemokine

[1]Corresponding author: Philip M. Murphy, M. D., Bldg 10, Room 11N111, NIH, Bethesda, MD 20892; Tel: 301-496-8616; Fax: 301-402-4369; pmm@nih.gov.

1. Introduction

CYTL1 (Cytokine-like protein 1; formerly known as C17) is a widely-expressed gene conserved from fish to man that encodes a 136 amino acid protein in humans. *CYTL1* expression was first identified in $CD34^+$ hematopoietic stem/progenitor cells from human cord blood, peripheral blood and bone marrow. It was originally thought to encode a cytokine because its expression in $CD34^+$ cells is dynamically regulated by immunoregulatory cytokines and growth factors, and because the encoded CYTL1 protein is small and secreted [1]. Subsequently, strikingly high *CYTL1* expression was found in chondrocytes [2,3] suggesting a role for *CYTL1* in cartilage biology. Consistent with this, a study of $Cytl1^{-/-}$ mice [4] identified autocrine/paracrine maintenance of cartilage homeostasis as the first cytokine-like activity of CYTL1, and suggested a role for CYTL1 in arthritis pathogenesis [4–6].

CYTL1 expression has since been found in many other normal tissues as well as in tumors, including benign prostatic hyperplasia [7], neuroblastoma and squamous cell carcinoma of the lung. CYTL1 was shown to positively regulate proliferation, migration and invasion of the neuroblastoma cell line SH-SY5Y *in vitro* [8]. In squamous cell carcinoma of the lung, CYTL1 expression is downregulated by hypermethylation of its promotor region compared to normal lung tissue [9].

In the Structural Classification of Proteins [10], cytokine-like proteins are classified into different folds based on their 3D structure, including the *4-helical cytokine* fold and the *IL8-like chemokine* fold. The rate of discovery of novel folds is very low (only 27 new folds in SCOP in the last 3 years [12]) compared to the number of newly solved structures in the PDB (29,792 new structures in the last 3 years [11]). Determining which fold CYTL1 adopts or whether it represents a novel fold is important for understanding in detail its mechanism of action. The protein sequence of CYTL1 lacks significant homology to any characterized sequences in public databases and therefore CYTL1 could not be classified into any 3D fold based on sequence similarity. Based on secondary structure prediction, CYTL1 was initially proposed to be a 4-helical cytokine [1]. Using computational fold recognition methods and atomic detail 3D models, we have previously performed a comprehensive search across more than 30,000 representative 3D structures to identify the best structural fit for CYTL1 among all possible known folds. Those studies predicted that, instead of a *4-helical cytokine* fold, CYTL1 may adopt a chemokine fold, most closely related to CCL2, the ligand for the chemokine receptor CCR2 [13]. This suggested that CYTL1 might regulate hematopoiesis and/or the immune response by functioning as a leukocyte chemoattractant. This was surprising since the spacing of the six cysteines found in CYTL1 differs from the canonical spacing patterns found for all members of the chemokine family. However, Wang *et al.* [14] have recently demonstrated specific high affinity CYTL1 binding (Kd=1 nM) to cell lines expressing the chemokine receptor CCR2b as well as potent chemotactic activity for mouse monocyte/macrophages isolated from wild type mice, but not from $Ccr2^{-/-}$ mice. Nevertheless, chemokines are defined by structure and chemokine receptors are able to bind many non-chemokine ligands, for example HMGB1, which binds to the chemokine receptor CXCR4. Therefore, direct characterization of the tertiary structure of CYTL1 is required to determine if it folds as a chemokine and therefore is a chemokine. Towards this goal, we

have developed a method for producing recombinant human CYTL1 in bacteria, and we provide new evidence that the biophysical and biochemical properties of CYTL1 are consistent cytokine-like properties with some overlap with and some distinction from the chemokines.

2. Materials and Methods

2. 1. Protein expression and purification of recombinant human CYTL1

A synthetic gene encoding the human CYTL1 protein (codons 20–136 lacking the signal peptide) fused to a C-terminal 6xHis-tag was cloned into the pNAN vector obtained from Blue Heron (Bothell, WA, USA). The resulting plasmid was transformed into *E. coli* strain OneShot BL21(DE3) (Invitrogen, Carlsbad, CA, USA) as well as endotoxin-free ClearColi BL21(DE3) (Lucigen, Middleton, WI, USA) for expression in inclusion bodies. The cells were grown at 37°C according to manufacturer's protocol and, when the optical density of the culture at 600 nm reached 0.6, recombinant protein expression was induced with 0.5 mM isopropyl-β-d-thiogalactopyranoside for 3 h (16 h for ClearColi). Cells were harvested by centrifugation at 4,000×g and resuspended in lysis buffer (100 mM Tris-HCl pH 8.0, 150 mM NaCl, 1% NP-40, 0.1% [wt/vol] sodium deoxycholate). Lysozyme was added to the cells for lysis by freezing and thawing. Multiple washes using centrifugation and resuspension were performed to purify the inclusion bodies. After the final wash, the pellet was dissolved in 50 mM Tris-HCl, 6 M guanidine-HCl, 1 mM EDTA, 1 M Urea and 1 mM dithiothreitol. The optimal refolding condition needed to achieve a high protein yield was found to be rapid dilution of CYTL1 inclusion bodies in refolding buffer containing 50 mM Tris-HCl pH 10, 50 mM NaCl, 500 mM arginine-HCl, 2 mM EDTA, 40 mM sucrose, 2 mM dithiothreitol and 5 mM cystamine. After stirring for 18 h at 4°C, the refolded protein was dialyzed two times against 12 L of 10 mM Tris-HCl pH 10. The protein was filtered through a 0.22-μm membrane, and purified by His-tag affinity chromatography using a 5 mL HisTrap HP nickel affinity column (GE healthcare, Marlborough, MA, USA) using 20 mM Tris-HCl pH 9.5, 500 mM NaCl and 20 mM imidazole as binding buffer, and 20 mM Tris-HCl pH 9.5, 500 mM NaCl and 500 mM imidazole as elution buffer. For biophysical analysis, CYTL1 was further purified by size exclusion chromatography on a Superdex 75 (GE healthcare, Marlborough, MA, USA) pre-equilibrated with 20 mM Tris-HCl pH 9.5, 150 mM NaCl. The peak protein fractions were pooled, but aggregation prevented concentration of CYTL1. Therefore, we added CHAPS to the dilute solution before concentration. We incubated the concentrated protein overnight at 4°C for equilibration in the final storage buffer of 20 mM Tris-HCl pH 9.5, 150 mM NaCl and 10 mM CHAPS. Afterwards, it was stored at −80°C until use. Protein concentrations were measured by absorption at 280 nm.

Endotoxin removal—Since the concentrated CYTL1 protein solution expressed in *E. coli* BL21(DE3) cells still contained high concentrations of endotoxin, we tried to remove endotoxin from CYTL1 before performing cell assays. We tested two different endotoxin extraction methods: Triton X-114 phase separation as previously described [15] and endotoxin removal spin columns (Pierce, No. 88276) according to the manufacturer's instructions.

In addition, by expressing CYTL1 in the genetically modified *E. coli* strain ClearColi BL21 (DE3) (Lucigen) that does not express endotoxin on its membrane, we were able to circumvent endotoxin contamination of CYTL1. Even though the protein yield was lower, we obtained protein suitable for functional assays. To avoid external endotoxin contamination during the purification, the size exclusion step was replaced by ion exchange chromatography (final buffer: 20 mM Tris-HCl pH 9.5, 250 mM NaCl). The peak CYTL1 fractions were pooled, concentrated in the presence of 10 mM CHAPS and sterile filtered prior to functional assays.

2. 2. Biophysical analysis of CYTL1

N-terminal sequencing: The purity and recovery of recombinant protein was confirmed by SDS-PAGE, subsequent transfer to a 0.22 μm PVDF membrane and *N*-terminal sequencing of the right size band of the protein on the gel. Dynamic Light Scattering: The particle size of the CYTL1 protein solution was measured by dynamic light scattering on a Zetasizer Nano S (Malvern Instruments, Westborough, MA, USA) at 25°C after 2 minutes pre-equilibration time (water viscosity 0.887 cP). Circular Dichroism (CD) spectra in the far UV-range (wavelength 195–260 nm) were obtained on a Jasco J-815 Circular Dichroism Spectropolarimeter (Jasco, Easton, MD, USA). We used a cuvette of 1 mm path length and a protein concentration of 3–6 μM at 20°C in 20 mM Tris, pH 8. The resulting spectra were the average of 5 repetitive scans at a scan rate of 50 nm/min, a bandwidth of 2 nm and a response time of 4 s. The CYTL1 secondary structure composition was calculated from the protein CD spectrum using the CAPITO webserver [16] (http://capito.nmr.fli-leibniz.de/index.php) after subtracting the CD spectrum of the buffer.

2. 3. Protein function analyses

Heparin binding—We studied the heparin binding potential of CYTL1 by heparin affinity chromatography using a 1 mL HiTrap Heparin HP column (GE Healthcare), with binding buffer: 20 mM Tris-HCl pH 9.5, 10 mM CHAPS; the elution buffer was the binding buffer with the addition of 1 M NaCl. CYTL1 was dialyzed into binding buffer to remove salt from the sample before loading it on the heparin sepharose column. The column was eluted using a continuous linear gradient from 0 to 1 M NaCl.

Chondrocyte Cell Culture—Human articular chondrocytes (HC-a) were obtained from ScienCell (Cat. #4650, Carlsbad, CA, USA) and maintained in Chondrocyte Medium (CM, ScienCell Cat. #4651). As chondrocytes are known to dedifferentiate in prolonged cell culture, the chondrocytes were frozen after the first passage in Cell Freezing Medium (Cat. #0133, ScienCell, Carlsbad, CA, USA) and a new culture was initiated from a fresh frozen stock before each experiment to ensure similar age of cells.

Chondrocyte RNA extraction and quantitative Real Time PCR (qRT-PCR)—For RNA extraction, cells were seeded into 6-well plates at a density of 19,000 per cm^2 (180,000 cells per well in 6 well plates) and incubated overnight (18 h) in a humidified incubator (37°C, 5% CO_2). The next day, cells were washed with PBS, and Low Serum Medium (LSM) containing various concentrations of cytokines (CYTL1: 50 nM, 100 nM, 500 nM, and CXCL12: 100 nM) was added to each well (LSM: Dulbecco's modified Eagle's

medium (DMEM, Cat. # 11995065, Gibco, Waltham, MA, USA) with 0.5% (v/v) fetal bovine serum (FBS, Cat # 16000036, Gibco), 100 μg/ml streptomycin, 100 I.U./ml penicillin (Cellgro # 30-002-CI, Corning, NY, USA). To isolate total RNA after 3 h and 24 h incubation with cytokines, chondrocytes were trypsinized and collected as a cell pellet prior to lysis with the RNeasy Mini Kit (Qiagen, Venlo, Netherlands) according to the manufacturer's instructions using Spin Technology. All samples contained between 200,000 – 400,000 cells in the pellet.

RNA extracted from cultured chondrocytes was reverse transcribed using the SensiFAST™ cDNA Synthesis Kit (Bioline, Taunton, MA, USA). Table 1 summarizes the primers used for amplification. qRT-PCR was performed using PerfeCTa SYBR Green FastMix, ROX (Quanta Biosciences, Beverly, MA, USA) on a 7900HT Fast Real-Time PCR System (Applied Biosystems, Foster City, CA, USA) in duplicates for 14 Genes (*CYTL1, Coll10A, SOX9, MMP13, IL-1β, ACAN, CXCR4, CCR2, IL6, MMP1, NAGLU, COL1A, COMP, CTS*) and two significantly upregulated genes, *CXCR4* and *CCR2*, were validated in four and eight replicates, respectively. The PCR cycling protocol started with 5 minutes of denaturation at 95°C, 40 cycles of 10 seconds at 95°C, and 30 seconds of extension at 60°C. We measured cycle threshold (CT) values, which denote the number of cycles required for the fluorescent signal to increase above background. The CT values of the target gene replicates were normalized to the median CT value of GAPDH replicates. Median gene expression fold changes, standard error of the mean (SEM) and p-values were calculated from the CT difference between non-treated and cytokine-treated replicates.

Chondrocyte calcium flux assays—Chondrocytes in Chondrocyte Medium were seeded into 96-well plates at a density of 50,000 cells per well and incubated overnight (18 h) in a humidified incubator (37°C, 5% CO_2). Cells were washed with PBS, incubated for 3 h in DMEM without FBS, and transferred into HBSS with 20 mM HEPES for 1 h. Then, the Calcium 4 assay component A was added, and incubated for 1 h before measurement of the calcium flux induced by different concentrations of cytokines (CYTL1: 50 nM, 100 nM and 150 nM) on a FlexStation 3 Multi-Mode Microplate Reader (Molecular Devices, Sunnyvale, CA, USA). The median of the first 10 measurements was subtracted from each data point to move the curves to the common start point at 0 RFU. We plotted the moving average of 5 data points to reduce fluctuations of the curves.

2. 4. Phylogenetic analysis of CYTL1 and the chemokine family

We generated a multiple sequence alignment of the chemokine family in Jalview version 2.10.1 [17] using Clustal with default parameters and the BLOSSUM30 substitution matrix [18] after removing the signal peptides from the protein sequences. Clustal requires some sequence similarity to properly align proteins, which is very low for CYTL1. Therefore, we inserted our structure-based alignment of CYTL1 with CCL2 generated in our previous study [13] manually and adjusted the chemokine family alignment accordingly (see alignment in Supp. Data 1). The phylogenetic tree was generated with the method *Average Distance using percent identity* in Jalview. The resulting tree was plotted as a right ladderized rectangular phylogram with Dendroscope 3.5.7 [19].

3. Results

Our goal was to investigate whether CYTL1 could be a member of the chemokine protein family. Thus, we compared biophysical and functional properties of the recombinantly expressed human CYTL1 protein with known chemokines. Our results indicate that CYTL1 has several chemokine-like properties.

3. 1. Recombinant human CYTL1 oligomerizes at higher concentrations

We successfully expressed Cytl1 protein in two different bacterial strains, with higher yield than most previously described mammalian expression systems [1,2,5]. Our yields from a 1-liter culture of E. coli BL21(DE3) were ~6 mg after His-tag affinity chromatography and ~0.6 mg after size exclusion chromatography. The yields from a 1-liter culture of ClearColi were ~0.4 mg Cytl1 after His-tag affinity chromatography and ~0.08 mg after ion exchange chromatography. These amounts are comparable to the best yield of 1 mg per liter culture reported for human CYTL1 in a CHO-based expression system [20].

Some proteins, including chemokines and *4-helical cytokines*, are known to oligomerize or aggregate under native-like conditions [21,22], which could interfere with subsequent experimental studies. Therefore, we studied recombinantly expressed human CYTL1 using dynamic light scattering, which measures the hydrodynamic size and size distribution of molecules and particles (by monitoring their Brownian motion with light scattering), and thus, gives information about the oligomeric or aggregation states of the protein. At concentrations of 0.5 mg/mL (~30 μM), CYTL1 formed higher order oligomers/aggregates with a particle radius of >900 nm (Fig. 1: blue graph). Further concentration of the protein solution was not possible due to visible precipitation that clogged the membrane of the concentrator device. To avoid this, we tested buffer conditions using various pH, salt and detergent concentrations. We found that with the addition of 10 mM CHAPS, the existing aggregates/large oligomers dissolved and CYTL1 remained in solution as it was concentrated to 5 mg/mL (~300 μM). In the presence of 10 mM CHAPS, CYTL1 is relatively monodisperse with a polydispersity index (an estimate of the broadness of the size distribution calculated from the cumulants analysis) of 0.26, and its particle radius of 2.4 – 3.2 nm measured by dynamic light scattering (Fig. 1: red graph) indicates that it likely forms dimers or tetramers. Since CHAPS is a relatively mild detergent, we used it to reduce aggregation and to keep CYTL1 in solution for further concentration in samples used for cell assays.

3.2. CYTL1 has secondary structure content similar to chemokines

Circular dichroism (CD) spectroscopy gives information about the secondary structure content (SSC) of proteins. Previously, we used computational fold recognition methods to predict the 3D structure of CYTL1 as an *IL8-like chemokine* fold and not as a *4-helical cytokine* fold [13] (Supp. Table 1).

Here, we measured the CYTL1 CD spectrum (Fig. 2A) and used it to derive secondary structure content by analytical methods available through the CAPITO Webserver [16] in order to compare our measured results with the computational predictions. CAPITO offers

two different methods for secondary structure estimation. The 'basis spectra' method extracts information from a calculated set of basis spectra, and the 'similar hits with lowest area difference' method is a matching-based approach calculating the lowest area difference to CD spectra of similar proteins from a reference dataset of known structure. Both methods derived similar results for the CYTL1 CD spectrum. CAPITO's secondary structure estimation via the basis spectra (Fig. 2B: red) with 13% alpha helix, 32% beta-strand and 46% irregular structure meets the content necessary to adopt a chemokine fold (Fig. 2B: yellow, ≥ 8% helix, ≥ 15% beta-strand) but lacks sufficient alpha-helix content to adopt a *4-helical cytokine* fold (only 13% helix measured, versus at least 34% necessary for a *4-helical cytokine* fold) (Fig. 2B: blue). Similarly, the estimated range of secondary structure content of CYTL1 using the lowest area difference method (Fig. 2C: red, 10–33% helix, 15–44% beta-strand) indicates that it does not have sufficient helical content to adopt a *4-helical cytokine* fold, but does meet the content required for an *IL8-like chemokine* fold. Nevertheless, other novel folds are possible.

3. 3. CYTL1 has low affinity to heparin at physiological salt conditions

It is known that many chemokines interact with glycosaminoglycans (GAGs) such as heparin. Therefore, we studied the heparin binding potential of CYTL1 by heparin affinity chromatography (Fig. 3). Compared to the total amount loaded, ~ 38 % of the protein did not bind to the column and was recovered in the flow through. Approximately, 25 % of the CYTL1 protein bound to the column and was recovered after elution with the salt gradient at concentrations between 100 – 300 mM NaCl, which is around the physiological salt concentration of 154 mM NaCl. Since not all CYTL1 protein was eluted from the column at 1 M NaCl, some CYTL1 protein might have bound more tightly to heparin. However, CYTL1 tends to aggregate more at low salt concentrations, and salt had to be removed from the buffer of the sample before loading it on the heparin sepharose column. In addition, it has been previously shown that heparin binding induces chemokine oligomerization [23]. It is possible that the remaining 37% of the total loaded CYTL1 protein aggregated, and thus, stayed on the column.

3.4. CYTL1 treatment increases gene expression of chemokine receptors CXCR4 and CCR2 in chondrocytes

CYTL1 has been described as an autocrine/paracrine factor influencing cartilage homeostasis [2]. Thus, we tested whether cytokine/chemokine stimulation induces changes in gene expression of selected chondrocyte specific markers and chemokine receptors after 3 h and 24 h to identify immediate as well as slower indirect effects, respectively. Our initial screen of 14 gene transcripts (Table 1: CYTL1, COL10A1, SOX9, MMP13, IL-1β, ACAN, CXCR4. CCR2. IL6, MMP1, NAGLU, COL1A, COMP, CTS) showed significant changes upon stimulation for four of the tested genes: CYTL1, IL6, CCR2 and CXCR4 (Fig. 4 and data not shown). The two chemokine receptors, CCR2 and CXCR4, were selected for validation in additional replicates (Fig. 4 and Supp. Fig. 1). Treatment with 100 nM CYTL1 showed no significant expression change after 3 h but strongly upregulated both CCR2 and CXCR4 gene expression in chondrocytes after 24 h incubation (Fig. 4: blue: fold increase 7.5 and 7.2, respectively and p-values 2e-5 and 0.009. respectively). While CXCL12 treatment slightly increased expression of both chemokine receptors after 3 h (Fig. 4: fold

change CXCR4: 1.3 and CCR2: 1.8), neither change was statistically significant, and CXCL12 treatment had no effect after 24 h incubation. Interestingly, combined treatment with both CXCL12 and CYTL1 rapidly and durably enhanced upregulation of CXCR4 and CCR2 mRNA expression, after 3 h stimulation (Fig. 4: 2.6 and 2.7 fold increase, p-values: 2e-5 and 0.003) and after 24 h stimulation (1.9 and 2.1 fold increase, p-values: 0.003 and 0.002).

CYTL1 gene expression increased after stimulation with 100 nM CYTL1, and was significantly upregulated after 24 h. Compared to CYTL1 treatment, treatment with CYTL1/CXCL12 together resulted in a more rapid increase in CYTL1 gene expression (data not shown). IL-6 gene expression was first upregulated after 3 h in all three treatment conditions and then, significantly downregulated after 24 h for CYTL1 and CXCL12 treatments, but returned to baseline values for treatment with CYTL1 and CXCL12 together (data not shown).

3. 5. CYTL1 induces calcium flux in human chondrocytes

We next measured intracellular calcium flux in response to cytokine treatment (Fig. 5). Chondrocytes responded to ATP used as positive control, but did not respond to CYTL1 buffer used as negative control. Treatment with 50 nM CYTL1 induced a robust calcium flux response (Fig. 5: pink curve), higher than that of ATP (red curve), but with slower initial kinetics. Cell responsiveness to CYTL1 was dose-dependent and was saturated at 100 nM. Overall the calcium flux response to CYTL1 lasted much longer (> 380 s) than the ATP response (~ 150 s). To test whether the response was induced by something other than protein in the CYTL1 sample, such as endotoxin, we also treated chondrocytes with boiled 100 nM CYTL1, which only induced a small increase of the calcium signal compared to unboiled CYTL1. We also observed a decrease of the calcium response between earlier and later replicate measurements (Supp. Fig. 2). This might be due to aggregation of CYTL1 after dilution into HBSS buffer, which reduced the detergent concentration below the critical micelle concentration of 6–10 mM and thus, reversing its solubilizing effects [24].

3. 6. Phylogenetic analysis of CYTL1 and the chemokine family

CYTL1 is located on chromosome 4p16.2 (Fig. 6: top left), the same chromosome where the large CXCL cluster is located at 4q21. While 3D structural studies would be necessary to establish whether CYTL1 folds as a chemokine, our previous modeling connection of CYTL1 to CCL2 and the recent report that CYTL1 is a CCR2b agonist justifies a phylogenetic analysis to compare cysteine patterns and possible disulfide bonds of CYTL1 when aligned with the chemokine family as the largest group of chemokine receptor ligands. The phylogenetic tree based on sequence identity shows that CYTL1 clusters far from typical CC or CXC chemokines and, therefore, has only very remote sequence homology to typical chemokines (Fig. 6: top right). Interestingly, CYTL1 forms a cluster with CXCL17, another chemokine with low sequence identity to typical chemokines and with atypical cysteine patterns and disulfide bonds (Fig. 6: bottom). CYTL1 shares the location and cysteine pattern of only disulfide bond formed by C-type/XCL# chemokines (Fig. 6: bottom). Furthermore, CYTL1 presents four additional cysteines that are sufficiently close to each other in the chemokine-like 3D model of CYTL1 to form additional disulfide bonds

(i.e. 2nd and 4th cysteine predicted previously [13]) or that have been observed at similar positions in 6C CC-type/CCL# chemokines (i.e. 5th and 6th cysteine [25]).

4. Discussion

We have developed a new protocol for production of recombinant His-tagged human CYTL1 protein in bacteria, and have shown using biophysical and biochemical methods that this atypical chemokine receptor ligand possesses some overlap and some distinctions with chemokines. In previous studies, CYTL1 protein was produced in mammalian expression systems [1,2,5] with relatively low yield, insufficient for biophysical or structural studies. Wang *et al.* [20] reported a more efficient mammalian expression system for CYTL1 production with a yield of 1 mg protein per liter of culture. However, this study did not provide evidence about whether all of the produced protein was in solution and functional in cell assays. We produced active CYTL1 protein in a bacterial expression system with a protein yield comparable to the method of Wang *et al.*

Purification of recombinant CYTL1 from *E. coli* has been challenging due to the tendency of CYTL1 to oligomerize and form aggregates, which increases with higher protein concentration, with reduced NaCl concentrations, or with lower pH conditions. Even though chemokine receptor binding and activation do not require chemokine oligomerization, most chemokines are known to form dimers, tetramers or higher order oligomers. For example, CCL3 and CCL4 form large rod-shaped, double-helical polymers [22]. Likewise, in solutions of purified CYTL1 protein, we detected large particles at concentrations above 30 μM (0.5 mg/mL). It is likely that oligomerization/aggregation is also occurring at lower CYTL1 concentrations but dynamic light scattering cannot reliably measure particle sizes below concentrations of 0.5 mg/mL. CYTL1 aggregation was reversible by the addition of 10 mM CHAPS, a zwitterionic detergent, and thus, we hypothesize that the aggregates are likely not caused by unfolding of CYTL1, but rather by interactions among its exposed surfaces. This is further supported by the fact that our CD results indicate formation of secondary structure elements even in the absence of salt or detergent in the sample. Both heparin binding and circular dichroism measurements required removal of salt from the sample, which likely resulted in an increase of oligomerization/aggregation. Heparin binding of chemokines has been shown to induce oligomerization [23]. Furthermore, previous studies found that the chemokine XCL1 (lymphotactin), which like Cytl1 only has one N-terminal cysteine residue, undergoes a fold switch in its dimer form that leads to higher affinity heparin binding but also to precipitation [26]. This fold switch of XCL1 results in observation of two heparin-sepharose elution peaks (one peak at 600 mM and a second peak at 900 mM NaCl [26]). Our dynamic light scattering results suggest that CYTL1 exists in an equilibrium of different oligomerization states. While our heparin binding results do not clearly indicate a domain switch, since only one elution peak is observed, it is still possible that only 25% of the CYTL1 sample adopted the right oligomeric state to weakly bind heparin, while the remaining 38% that was recovered in the flow-through might not expose the heparin binding site to enable tight binding to the column. The 37% of loaded protein that was not recovered might have bound more tightly. However, it is more likely that the unrecovered protein fraction has formed large oligomers that stayed on the column due to the low salt conditions or heparin-induced precipitation. The decrease of the Ca-flux signal

over time after dilution into HBSS buffer might have been caused by oligomerization/aggregation under the changed conditions, and thus, a monomeric (active) form of CYTL1 available for receptor interaction and binding may have decreased over time (Supp. Fig. 2). Further studies would be necessary to determine what biological purpose oligomerizarion serves; possibilities include signaling regulation at high concentrations, protein storage and degradation.

For proteins expressed in bacteria, endotoxin contamination may interfere with cell assays. Endotoxin, a component of the outer membranes of bacteria, induces a strong immune response in leukocytes even at low concentrations, which is detectable as Ca-flux. For CYTL1 in this study, the extraction of endotoxin was a problem. First, endotoxin extraction with the Pierce column caused a 50% loss of CYTL1 protein. Second, extraction of endotoxin by phase separation with Triton X-114 made the sample unsuitable for assays, as the Triton X-114 could not be completely removed, most likely due to mixed micelle formation with CHAPS. Therefore, for use in cell assays, we expressed and purified CYTL1 from endotoxin free ClearColi BL21(DE3) bacteria. The modified endotoxin of ClearColi cells has been shown not to induce an immune response. However, because the modified endotoxin cannot be distinguished from unmodified endotoxin by standard endotoxin assays, it was not possible to verify the absence of any endotoxin contamination.

So far, no calcium flux experiments in chemokine-stimulated chondrocytes have been reported in the literature. We observed that CYTL1 induces robust calcium flux responses in chondrocytes in a dose-dependent manner, similar to the concentration range observed for induction of calcium flux by chemokines in leukocytes. Interestingly, the signal persisted significantly longer than usually reported for chemokine signals, which typically return to baseline ~150 s after stimulation.

Furthermore, after CXCL12 stimulation, previous studies reported upregulation of protein expression and secretion of matrix proteases (MMP1, MMP13) and enzymes (CTSB, NAGLU) [27]. Although the RNA expression changes we observed after CXCL12 stimulation for those genes (MMP1, MMP13, NAGLU, CTSB) were not significant, there could still be significant changes in protein expression and/or secretion as were observed in earlier studies [27]. CYTL1 has been reported to downregulate RNA expression of the inflammatory markers IL-1β and IL-6 *in vivo* in arthritic joints of CYTL1 over-expressing mice [5]. While IL-1β downregulation was not significant in our experiment, we found that both CXCL12 and CYTL1 increased IL-6 RNA expression after 3 h, and then significantly downregulated IL-6 expression after 24 h (data not shown). IL-6 is known to stimulate inflammatory and autoimmune processes in many diseases including rheumatoid arthritis. Thus, IL-6 downregulation could contribute to the protective effect of CYTL1 observed in arthritic mice [28]. Interestingly, CYTL1 upregulates its own expression (data not shown) and through this mechanism may be able to further enhance its effects as a paracrine/autocrine signal over time. The strong upregulation of chemokine receptors CXCR4 and CCR2 by CYTL1 after 24 h but not after 3 h may indicate an indirect effect of CYTL1 on chemokine receptor expression, and both receptors may be important for proper chondrocyte function and immune surveillance in cartilage. Furthermore, not only CCR2 a recently reported receptor for CYTL1 but also CXCR4 may have a relationship with CYTL1

signaling. We observed for example that stimulation with both CYTL1 and CXCL12 increased CYTL1 RNA upregulation compared to CYTL1 alone and enhanced the chemokine receptor upregulation compared to CXCL12 alone. Interestingly, like CYTL1, CXCL12 is also highly expressed in CD34+ hematopoietic progenitor cells, which further suggests a possible functional relationship between those proteins or crosstalk through their receptors even in different cell types.

Interestingly, our phylogenetic analysis of CYTL1 and the chemokine protein family shows that CYTL1 clusters with CXCL17, another chemokine with low sequence identity to typical chemokines and with potential atypical cysteine patterns and disulfide bonds. Like CYTL1, CXCL17 was also not discovered by classical sequence-based alignment methods, but by fold recognition and molecular modeling methods [29]. CYTL1 clusters relatively far in the phylogenetic tree from CXC-type chemokines found on the same chromosome. Therefore, if CYTL1 was a remote homolog of the chemokine family, it may have split very early on or may have a different origin as CXC-type chemokines. The fact that CYTL1 has been found to bind to a CC-type chemokine receptor and presents additional cysteines after the C-terminal helix like 6C CC-type chemokines indicates that it may have evolved from CC-type chemokines.

Attempts to identify a receptor for CYTL1 were initially focused on various common gamma chain-related hematopoietic cytokine receptors, because of its initial prediction to belong to the *4-helical cytokine* family [5]. However, those attempts were unsuccessful and instead CCR2b has recently been demonstrated to be a functional receptor for CYTL1 [14]. This is consistent with our previous structure-based computational results, which showed that CYTL1 is most likely to fold like CCL2, the chemokine ligand for CCR2 [13]. Since chemokines are defined by structure, not function, and since non-chemokine ligands are well known to bind to chemokine receptors, additional experimental evidence is needed to validate CYTL1 as an atypical chemokine. The tendency to oligomerize or aggregate is a property of CYTL1 that is known for both chemokines and *4-helical cytokines*. However, the secondary structure content we measured is not in agreement with a *4-helical cytokine* fold, but is compatible with a chemokine-like fold. Still, it is important to mention that there could be other proteins showing similar properties including e.g. defensin-like peptides that have been shown to signal through chemokine receptors, while not presenting a chemokine-like tertiary structure, but similar secondary structure content [30]. Thus, definitive structural studies will be needed to determine whether CYTL1 adopts a chemokine fold.

5. Conclusion

Although CYTL1 has initially been proposed to adopt a *4-helical cytokine* fold, our previous modeling study provided statistical evidence that CYTL1 may adopt a chemokine-like fold [13]. The present analysis of recombinant CYTL1 protein produced in bacteria has identified several additional properties of human CYTL1 including a higher content of beta-sheet than alpha-helix secondary structure, induction of calcium-flux in chondrocytes and upregulation of chemokine receptor expression. Together with the recent discovery of CCR2b as a functional receptor for CYTL1, our results reinforce the general point that atypical cytokine-like proteins may be important functional ligands for chemokine receptors.

Supplementary Material

Refer to Web version on PubMed Central for supplementary material.

Acknowledgments

David Hall and Sergio M. Pontejo for helpful discussions.

Funding

This work was supported by the German Academic Exchange Service (DAAD) and the Intramural Research Program of the National Institute of Allergy and Infectious Diseases.

References

1. Liu X, Rapp N, Deans R, Cheng L. Molecular cloning and chromosomal mapping of a candidate cytokine gene selectively expressed in human CD34+ cells. Genomics. 2000; 65:283–92. [PubMed: 10857752]
2. Kim JS, Ryoo ZY, Chun JS. Cytokine-like 1 (Cytl1) regulates the chondrogenesis of mesenchymal cells. J Biol Chem. 2007; 282:29359–29367. DOI: 10.1074/jbc.M700965200 [PubMed: 17644814]
3. Hermansson M, Sawaji Y, Bolton M, Alexander S, Wallace A, Begum S, Wait R, Saklatvala J. Proteomic analysis of articular cartilage shows increased type II collagen synthesis in osteoarthritis and expression of inhibin betaA (activin A), a regulatory molecule for chondrocytes. J Biol Chem. 2004; 279:43514–21. [PubMed: 15292256]
4. Jeon J, Oh H, Lee G, Ryu JH, Rhee J, Kim JH, Chung KH, Song WK, Chun CH, Chun JS. Cytokine-like 1 knock-out mice (Cytl1−/−) show normal cartilage and bone development but exhibit augmented osteoarthritic cartilage destruction. J Biol Chem. 2011; 286:27206–27213. DOI: 10.1074/jbc.M111.218065 [PubMed: 21652695]
5. Chao C, Joyce-Shaikh B, Grein J, Moshrefi M, Raoufi F, Laface DM, McClanahan TK, Bourne PA, Pierce RH, Gorman DM, Pflanz S. C17 prevents inflammatory arthritis and associated joint destruction in mice. PloS One. 2011; 6:e22256.doi: 10.1371/journal.pone.0022256 [PubMed: 21799806]
6. Stenberg J, Rüetschi U, Skiöldebrand E, Kärrholm J, Lindahl A. Quantitative proteomics reveals regulatory differences in the chondrocyte secretome from human medial and lateral femoral condyles in osteoarthritic patients. Proteome Sci. 2013; 11:43.doi: 10.1186/1477-5956-11-43 [PubMed: 24090399]
7. Begley LA, Kasina S, MacDonald J, Macoska JA. The inflammatory microenvironment of the aging prostate facilitates cellular proliferation and hypertrophy. Cytokine. 2008; 43:194–199. DOI: 10.1016/j.cyto.2008.05.012 [PubMed: 18572414]
8. Wen M, Wang H, Zhang X, Long J, Lv Z, Kong Q, An Y. Cytokine-like 1 is involved in the growth and metastasis of neuroblastoma cells. Int J Oncol. 2012; 41:1419–1424. DOI: 10.3892/ijo.2012.1552 [PubMed: 22797702]
9. Kwon YJ, Lee SJ, Koh JS, Kim SH, Lee HW, Kang MC, Bae JB, Kim YJ, Park JH. Genome-wide analysis of DNA methylation and the gene expression change in lung cancer. J Thorac Oncol Off Publ Int Assoc Study Lung Cancer. 2012; 7:20–33. DOI: 10.1097/JTO.0b013e3182307f62
10. Andreeva A, Howorth D, Chothia C, Kulesha E, Murzin AG. SCOP2 prototype: a new approach to protein structure mining. Nucleic Acids Res. 2014; 42:D310–D314. DOI: 10.1093/nar/gkt1242 [PubMed: 24293656]
11. PDB. 2009. http://www.rcsb.org/pdb/statistics/contentGrowthChart.do?content=fold-scophttp://www.rcsb.org/pdb/statistics/contentGrowthChart.do?content=fold-scop
12. [accessed February 20, 2017] SCOPe 2.06: Structural Classification of Proteins — extended. n.d. https://scop.berkeley.edu/statistics/ver=2.06
13. Tomczak A, Pisabarro MT. Identification of CCR2-binding features in Cytl1 by a CCL2-like chemokine model. Proteins. 2011; 79:1277–1292. DOI: 10.1002/prot.22963 [PubMed: 21322034]

14. Wang X, Li T, Wang W, Yuan W, Liu H, Cheng Y, Wang P, Zhang Y, Han W. Cytokine-like 1 Chemoattracts Monocytes/Macrophages via CCR2. J Immunol Baltim Md 1950. 2016; 196:4090–4099. DOI: 10.4049/jimmunol.1501908
15. Aida Y, Pabst MJ. Removal of endotoxin from protein solutions by phase separation using Triton X-114. J Immunol Methods. 1990; 132:191–195. [PubMed: 2170533]
16. Wiedemann C, Bellstedt P, Görlach M. CAPITO--a web server-based analysis and plotting tool for circular dichroism data. Bioinforma Oxf Engl. 2013; 29:1750–1757. DOI: 10.1093/bioinformatics/btt278
17. Waterhouse AM, Procter JB, Martin DM, Clamp M, Barton GJ. Jalview Version 2--a multiple sequence alignment editor and analysis workbench. Bioinformatics. 2009; 25:1189–91. [PubMed: 19151095]
18. Larkin MA, Blackshields G, Brown NP, Chenna R, McGettigan PA, McWilliam H, Valentin F, Wallace IM, Wilm A, Lopez R, Thompson JD, Gibson TJ, Higgins DG. Clustal W and Clustal X version 2.0. Bioinformatics. 2007; 23:2947–2948. DOI: 10.1093/bioinformatics/btm404 [PubMed: 17846036]
19. Huson DH, Richter DC, Rausch C, Dezulian T, Franz M, Rupp R. Dendroscope: An interactive viewer for large phylogenetic trees. BMC Bioinformatics. 2007; 8:460.doi: 10.1186/1471-2105-8-460 [PubMed: 18034891]
20. Wang X, Liu H, Yuan W, Cheng Y, Han W. Efficient production of CYTL1 protein using mouse IgGκ signal peptide in the CHO cell expression system. Acta Biochim Biophys Sin. 2016; 48:391–394. DOI: 10.1093/abbs/gmw007 [PubMed: 26922322]
21. Raso SW, Abel J, Barnes JM, Maloney KM, Pipes G, Treuheit MJ, King J, Brems DN. Aggregation of granulocyte-colony stimulating factor in vitro involves a conformationally altered monomeric state. Protein Sci. 2005; 14:2246–2257. DOI: 10.1110/ps.051489405 [PubMed: 16131655]
22. Ren M, Guo Q, Guo L, Lenz M, Qian F, Koenen RR, Xu H, Schilling AB, Weber C, Ye RD, Dinner AR, Tang WJ. Polymerization of MIP-1 chemokine (CCL3 and CCL4) and clearance of MIP-1 by insulin-degrading enzyme. EMBO J. 2010; 29:3952–3966. DOI: 10.1038/emboj.2010.256 [PubMed: 20959807]
23. Rek A, Brandner B, Geretti E, Kungl AJ. A biophysical insight into the RANTES-glycosaminoglycan interaction. Biochim Biophys Acta. 2009; 1794:577–582. DOI: 10.1016/j.bbapap.2009.01.001 [PubMed: 19455751]
24. Chattopadhyay A, Harikumar KG. Dependence of critical micelle concentration of a zwitterionic detergent on ionic strength: implications in receptor solubilization. FEBS Lett. 1996; 391:199–202. [PubMed: 8706916]
25. Love M, Sandberg JL, Ziarek JJ, Gerarden KP, Rode RR, Jensen DR, McCaslin DR, Peterson FC, Veldkamp CT. Solution Structure of CCL21 and Identification of a Putative CCR7 Binding Site. Biochemistry (Mosc). 2012; 51:733–735. DOI: 10.1021/bi201601k
26. Tuinstra RL, Peterson FC, Kutlesa S, Elgin ES, Kron MA, Volkman BF. Interconversion between two unrelated protein folds in the lymphotactin native state. Proc Natl Acad Sci U A. 2008; 105:5057–62.
27. Mazzetti I, Magagnoli G, Paoletti S, Uguccioni M, Olivotto E, Vitellozzi R, Cattini L, Facchini A, Borzì RM. A role for chemokines in the induction of chondrocyte phenotype modulation. Arthritis Rheum. 2004; 50:112–122. DOI: 10.1002/art.11474 [PubMed: 14730607]
28. Nishimoto N. Interleukin-6 in rheumatoid arthritis. Curr Opin Rheumatol. 2006; 18:277–281. DOI: 10.1097/01.bor.0000218949.19860.d1 [PubMed: 16582692]
29. Pisabarro MT, Leung B, Kwong M, Corpuz R, Frantz GD, Chiang N, Vandlen R, Diehl LJ, Skelton N, Kim HS, Eaton D, Schmidt KN. Cutting edge: novel human dendritic cell- and monocyte-attracting chemokine-like protein identified by fold recognition methods. J Immunol. 2006; 176:2069–73. [PubMed: 16455961]
30. Yang D, Chertov O, Bykovskaia SN, Chen Q, Buffo MJ, Shogan J, Anderson M, Schröder JM, Wang JM, Howard OM, Oppenheim JJ. Beta-defensins: linking innate and adaptive immunity through dendritic and T cell CCR6. Science. 1999; 286:525–528. [PubMed: 10521347]

31. Wittamer V, Gregoire F, Robberecht P, Vassart G, Communi D, Parmentier M. The C-terminal Nonapeptide of Mature Chemerin Activates the Chemerin Receptor with Low Nanomolar Potency. J Biol Chem. 2004; 279:9956–9962. DOI: 10.1074/jbc.M313016200 [PubMed: 14701797]

Highlights

- CYTL1 has secondary structure content that is not consistent with a *4-helical cytokine* fold but is similar to known chemokines.
- CYTL1 induces calcium flux in human chondrocytes.
- CYTL1 appears to be an atypical chemokine receptor ligand.

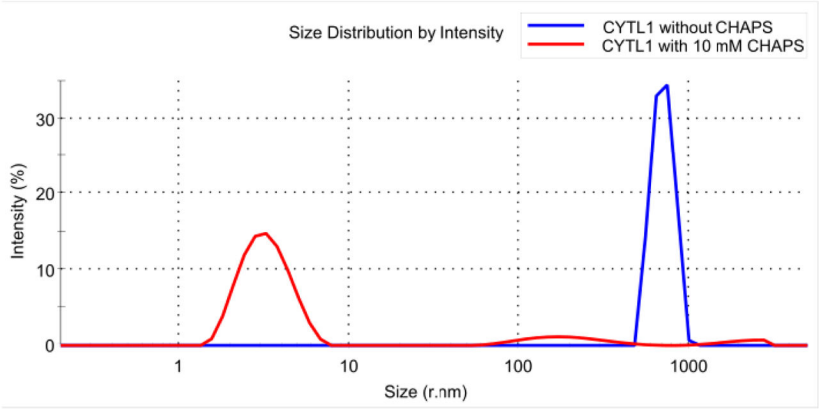

Fig. 1. Recombinant CYTL1 oligomerizes at concentrations >0.5 mg/mL

Dynamic light scattering of CYTL1 without CHAPS (blue, concentration 0.5 mg/mL) and with 10 mM CHAPS (red. 5mg/mL). Data are representative of four independent experiments.

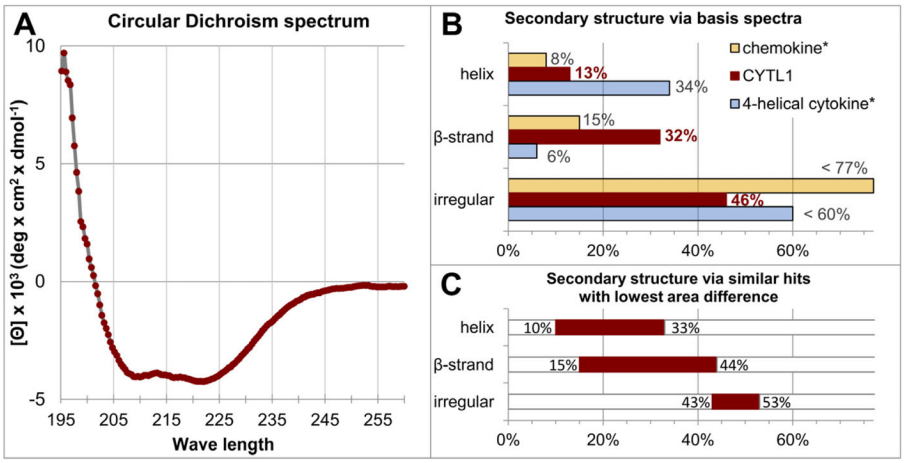

Fig. 2. Recombinant CYTL1 has secondary structure similar to chemokines, but not to *4-helical cytokines*

Circular dichroism and derived secondary structure percentages of CYTL1. **A)** CYTL1 circular dichroism spectrum. **B)** CYTL1 secondary structure fractions derived from the basis spectra method using CAPITO [16] (http://capito.nmr.fli-leibniz.de/index.php) in comparison to secondary structure predicted by 3D modeling of CYTL1 as an *IL8-like chemokine* versus a *4-helical cytokine* fold. * predicted percentages derived from 3D models of CYTL1 [13]: as chemokine (helix: ≥12 amino acids (AA), β-strand: ≥19 AA) or *4-helical cytokine* (helix: ≥ 46 AA, β-strand: ≥ 8 AA). **C)** CYTL1 secondary structure fraction ranges derived from CD spectrum via similar hits with lowest area difference using CAPITO. Data are representative of two independent CD experiments.

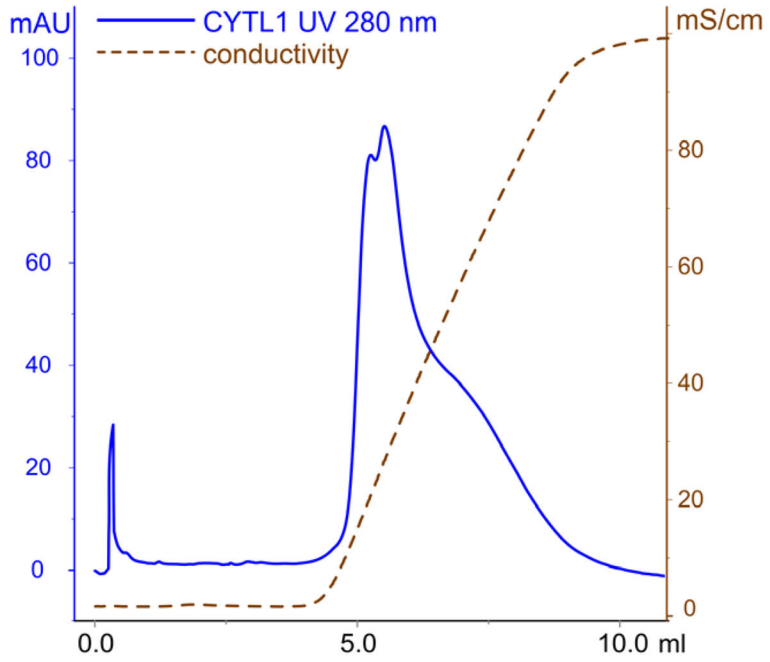

Fig. 3. Recombinant CYTL1 binds heparin. Elution profiles for CYTL1 (blue) from heparin-sepharose with increasing conductivity (brown) due to increasing NaCl concentration

Data are from a single experiment.

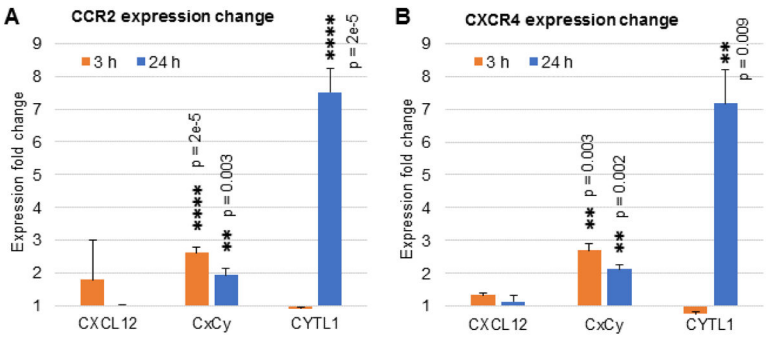

Fig. 4. Recombinant CYTL1 upregulates chemokine receptor gene expression in human chondrocytes

Comparison of changes in gene expression induced by treatment with 100 nM CYTL1, 100 nM CXCL12 or both at the same time (denoted as CxCy) after 3 h (orange) and 24 h (blue) incubation in chondrocytes for the following genes: **A)** *CCR2*, **B)** *CXCR4*. Error bars denote standard error of the mean (SEM), p-value labels: **** $p < 0.0001$, *** $p < 0.001$, ** $p < 0.01$, * $p < 0.05$, no label: not significant. Data are representative of 2 independent experiments, mean of 4–8 replicates shown.

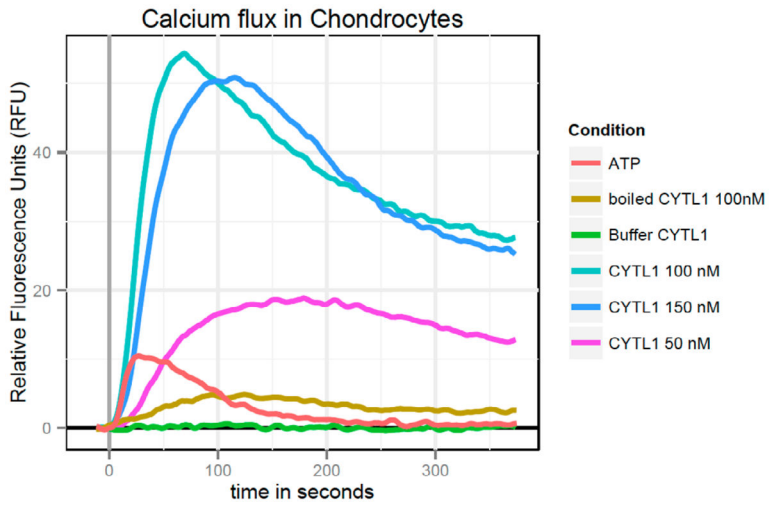

Fig. 5. Recombinant CYTL1 induces calcium flux in cultured human chondrocytes

CYTL1 and controls were added at time=0 s. Data are representative of 3 independent experiments in which each condition was tested in 2–6 replicates.

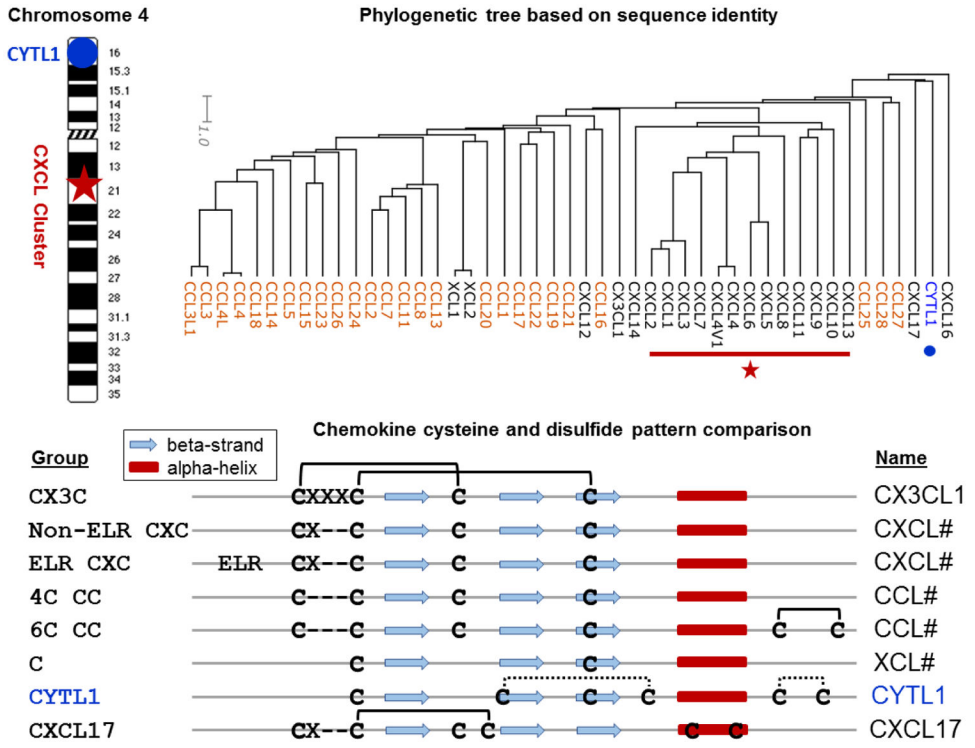

Fig. 6. Phylogenetic analysis of CYTL1 (blue) and the chemokine family

Top: The chromosomal location of CYTL1 (blue circle) and other chemokines (red star) on chromosome 4 (left) and their position in the phylogenetic tree of the chemokine family (right) show that CYTL1 has only very remote homology to typical chemokines and clusters with CXCL17. **Bottom:** Comparison of cysteine patterns and disulfide bond formation in typical chemokines and CYTL1 (blue). Alpha-helix secondary structure in red, beta-sheet in blue and cysteines and disulfide bonds in black, dotted lines indicate putative disulfide bonds in CYTL1. CYTL1 shares the bond formed by C-type/XCL# chemokines, and presents additional cysteines that may form additional disulfide bond(s) as they come close in the chemokine-like 3D model of CYTL1 (2^{nd} and 4^{th} cysteine) or have been proposed to form a bond in 6C CC-type/CCL# chemokines (5^{th} and 6^{th} cysteine).

Table 1

Primers used for qRT-PCR of cytokine treated chondrocytes.

Primer ID	Sequence	Product size	Name
FH1_CXCR4 RH1_CXCR4	5′-AACTTCAGTTTGTTGGCTG-3′ 5′-GTGTATATACTGATCCCCTCC-3′	118 bp	Chemokine receptor CXCR4
FH1_CCR2 RH1_CCR2	5′-AAGCCTTTTTCACATAGCTC-3′ 5′-CTTTCACATTCTTTCCTGGTC-3′	95 bp	Chemokine receptor CCR2
FH1_GAPDH RH1_GAPDH	5′-ACAGTTGCCATGTAGACC-3′ 5′-TTTTTGGTTGAGCACAGG -3′	95 bp	Glyceraldehyde-3-phosphate dehydrogenase (GAPDH)
FH1_CYTL1 RH1_CYTL1	5′-CACAGGTCTTGTGTTAGTTG-3′ 5′-TAGTGACCAAATCAACATGC-3′	181 bp	Cytokine-like 1 (CYTL1)
FH1_IL6 RH1_IL6	5′-GCAGAAAAAGGCAAAGAATC-3′ 5′-CTACATTTGCCGAAGAGC-3′	178 bp	Interleukin 6

Sigma Predesigned SYBR® Green I Primers for RT-qPCR, PrimerPair IDs: H_CYTL1_1, H_GAPDH_1, H_COL10A1_1, H_SOX9_1, H_MMP13_1, H_IL1B_1, H_ACAN_1, H_CXCR4_1, H_CCR2_1, H_IL6_1, H_MMP1_1, H_MMP3_1, H_COL1A2_1, H_COL2A1_1, H_IGF1_1, H_NAGLU_1 H_COMP_1, H_CTSB_1